Supplementary Information

Potential-driven restructuring of lithium cobalt oxide yields an enhanced active phase for the oxygen evolution reaction

Alexander A. Ryabin‡ [a,b], Subin Choi‡ [a], Yumin Heo‡ [a], Sebastian Kunze [a], Dmitry V. Pelegov*[b] and Jongwoo Lim *[a]

[a] Department of Chemistry, Seoul National University, Seoul, 08826, Republic of Korea.

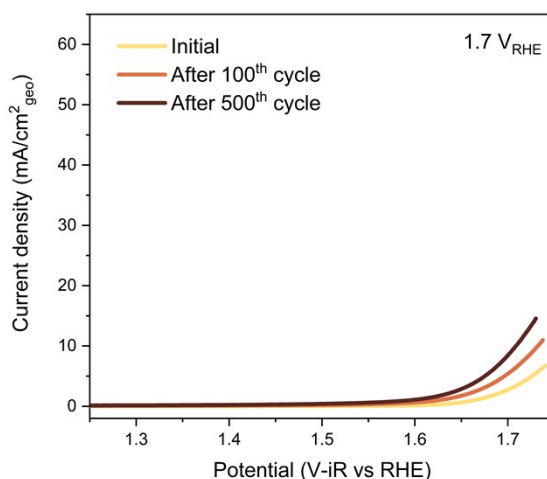[b] Institute of Natural Sciences and Mathematics, Ural Federal University, Yekaterinburg 620002, Russia

Fig. S1 Linear sweep voltammogram of $LiCoO_2$ cycled up to 1.7 V_{RHE} after different number of CV cycles.
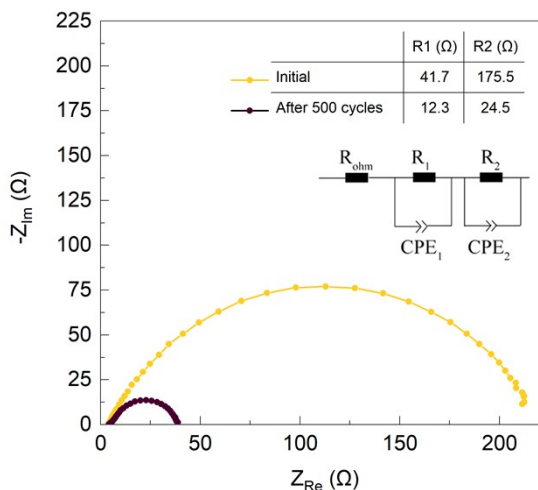

Fig. S2 Electrochemical impedance spectroscopy of $LiCoO_2$ before and after 500 cycles up to 1.8 V_{RHE}.

Electrochemical impedance spectroscopy (EIS) measurements were measured at a potential of 1.70 V versus RHE in a frequency range from 200 kHz to 0.5 Hz with an amplitude of 10 mV. In equivalent circuit used for the fitting of the EIS responses R_{ohm}, R_1, R_2, CPE_1, and CPE_2 represent the solution resistance, electrode texture and charge transfer resistances, and constant phase elements, respectively.
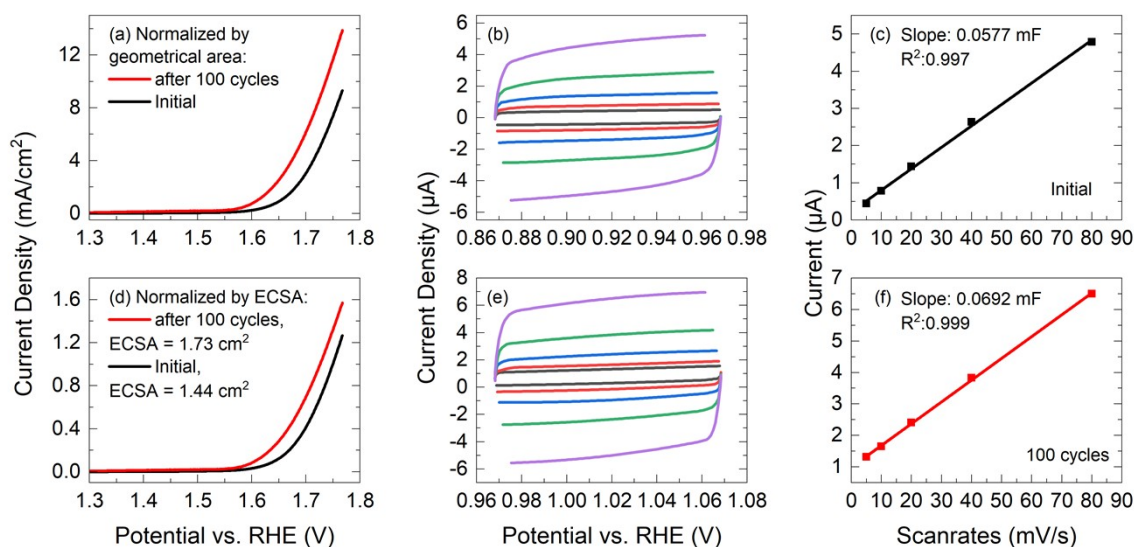
Fig. S3 Electrochemical performance of LCO normalized by geometrical area (a) and ECSA (d). CV curves measured in a non-Faradaic region of the voltammogram before (b) and after 100 cycles (e). The dependence of the capacitive current on the different potential scan rates before (c) and after 100 cycles (f).

For the ECSA experiment, the sample was prepared as follows: 2 mg of $LiCoO_2$ powder was dispersed in a solution containing 0.49 mL of isopropyl alcohol and 0.49 mL of deionized water, which was then sonicated for 20 minutes until a uniform dispersion was achieved. Subsequently,10 μL of Nafion solution (5%) was added to the mixture and sonicated continuously for an additional 20 minutes to ensure homogeneity. Three aliquots of 10 μL each were then deposited onto a polished glassy carbon electrode with a loaded area of 0.196 cm^2. Finally, the sample was dried at room temperature.
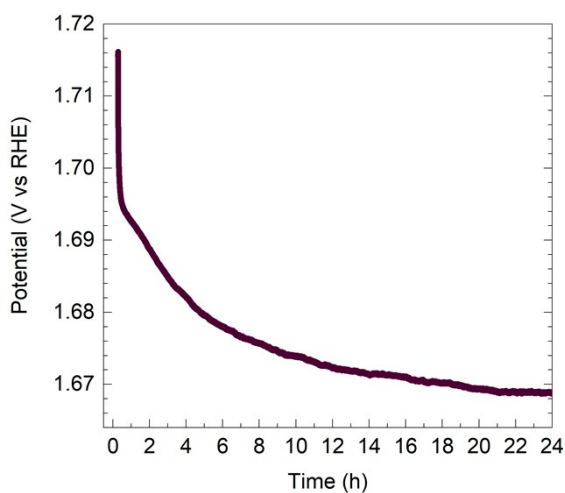

Fig. S4 Chronopotentiometry test at 10 mA cm^{-2} of LCO@1.8 after 500 cycles.
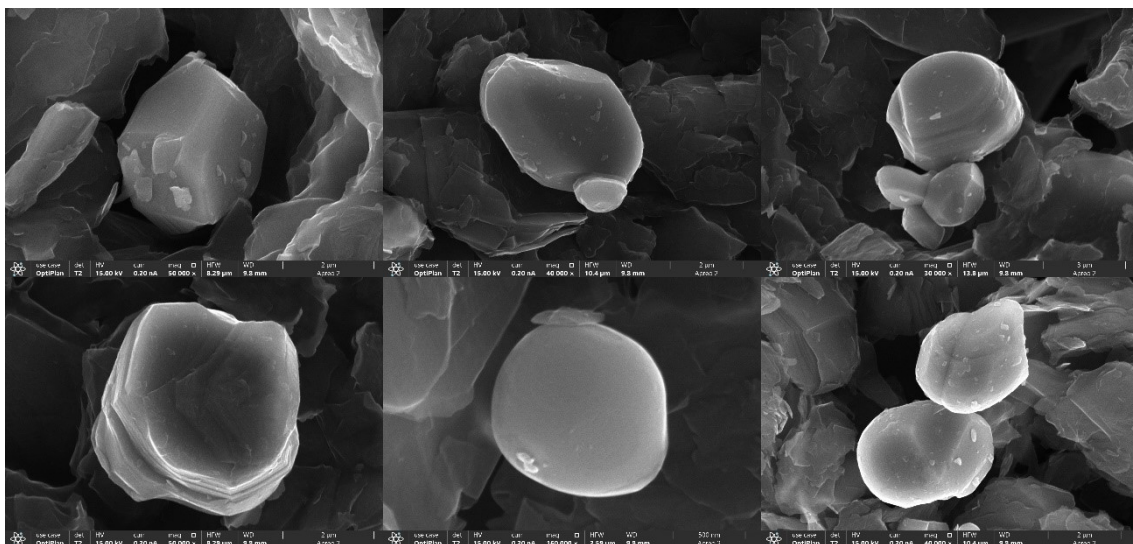
Fig. S5 FE-SEM images of a LCO particle deposited on carbon paper before cycling.
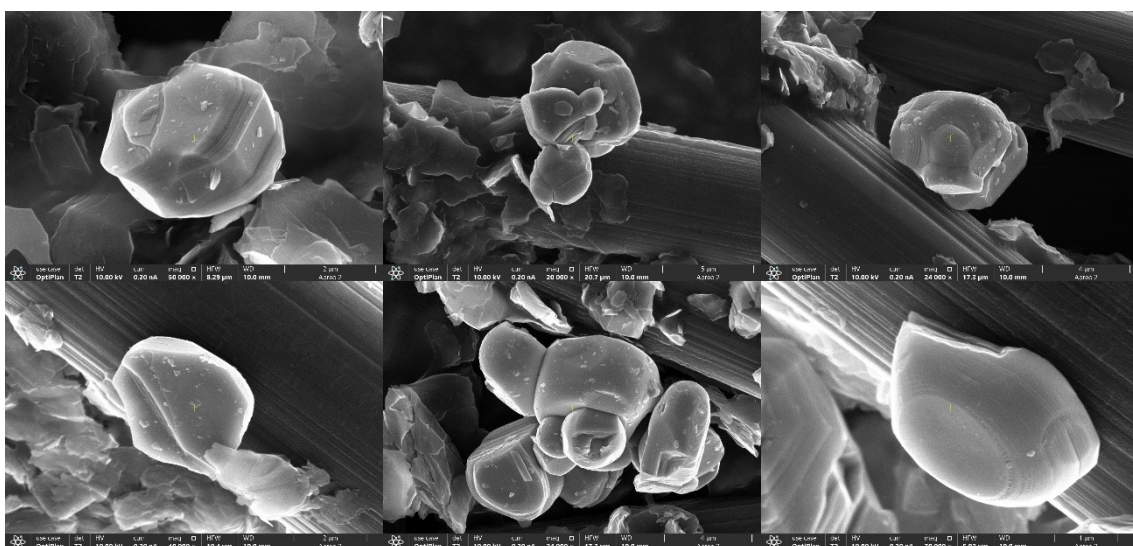

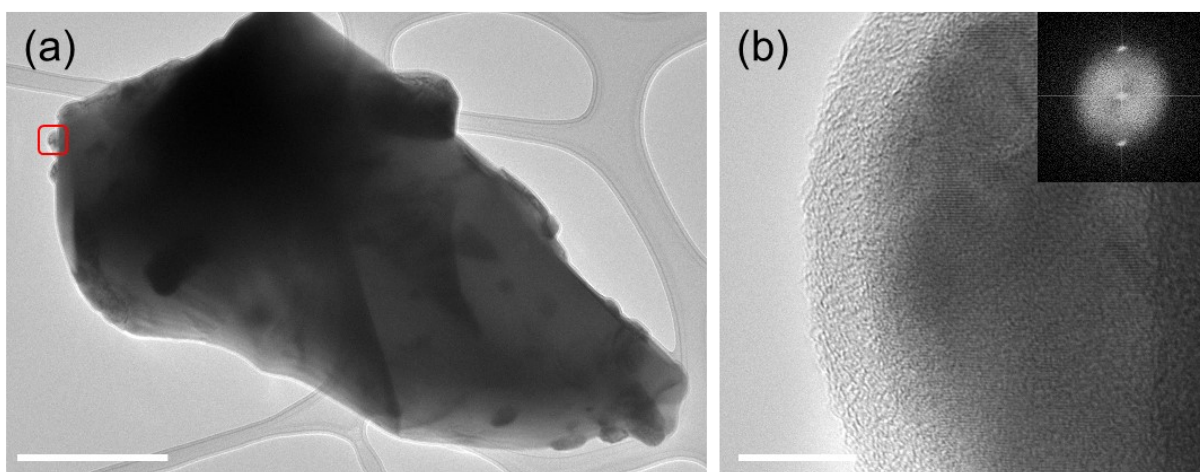**Fig. S6** FE-SEM images of a LCO@1.8 particle after 500 cycles.

Fig. S7 (a)-(b) TEM image of LCO@1.8 after 50 cycles. The scale bar in (a) and (b) represents 500 nm and 10 nm, respectively.
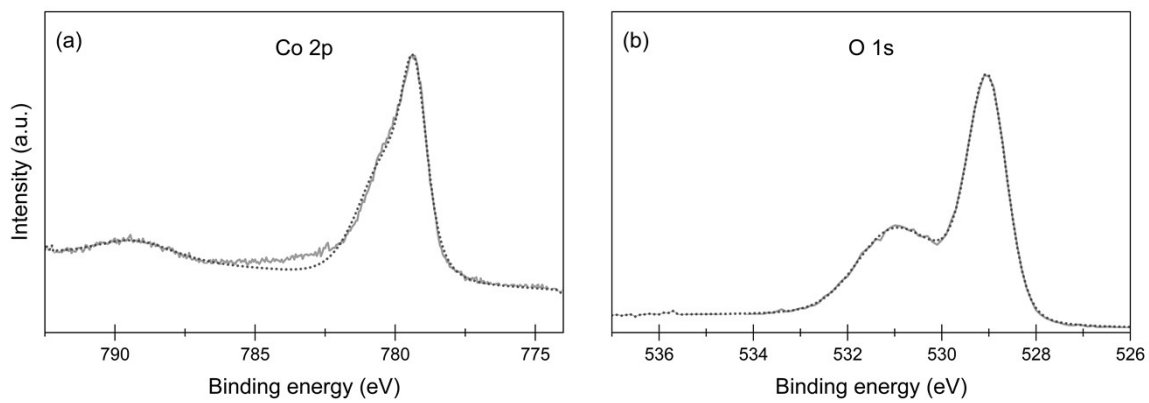
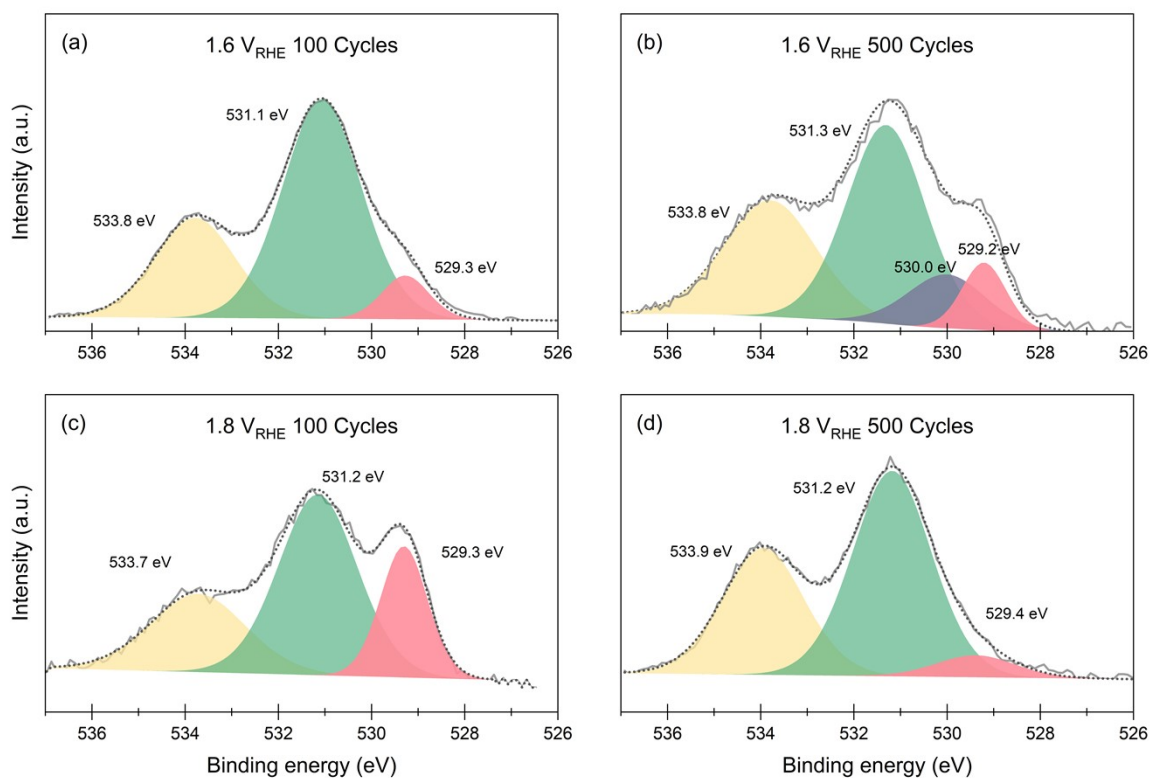**Fig. S8** (a) Co 2p and (b) O 1s XPS spectra of pristine LCO.

Fig. S9 O 1s XPS spectra of (a) 1.6 V_{RHE} 100 Cycles, (b) 1.6 V_{RHE} 500 Cycles, (c) 1.8 V_{RHE} 100 Cycles, and (d) 1.8 V_{RHE} 500 Cycles.

In LiCoO$_2$, lithium diffusion in the *ab*-plane is faster compared to lithium transfer across the CoO$_2$ layers (along the *c*-axis).[1] Therefore, LCO particles with a preferable hexagonal shape might exhibit a higher degree of delithiation on the edges of the *ab*-plane, forming a donut-shaped particle. Due to the higher surface area in the ab-plane of such particles, they might preferentially deposit onto the substrate with this side facing down. In this case, the *c*-axis of the crystal structure will be aligned with the *z*-axis of the laboratory system. This series of assumptions provides an alternative model to explain the Raman line scan signal profile. However, we suspect that even in this scenario, there should be a small delithiation layer on the top and bottom of the particle, resulting in a core-shell particle with a non-uniform width of the shell.
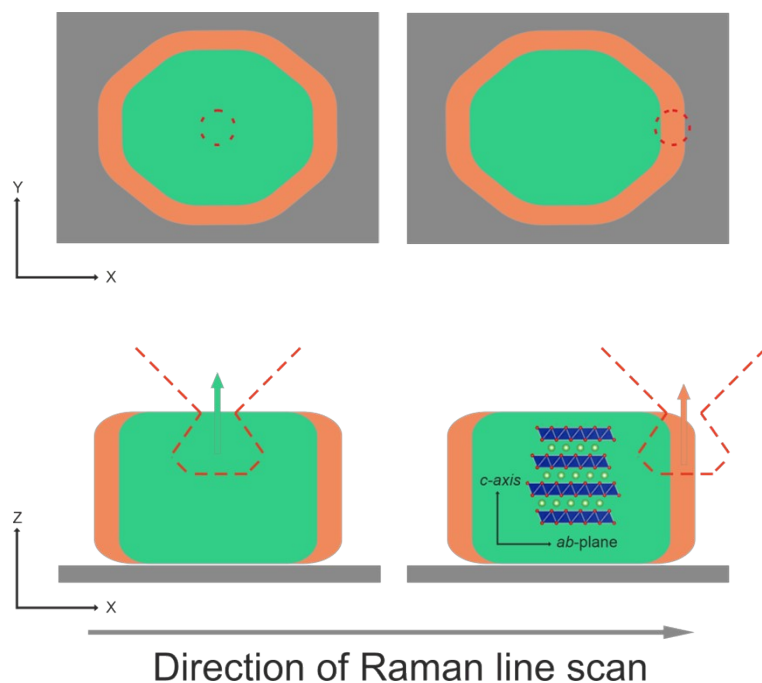

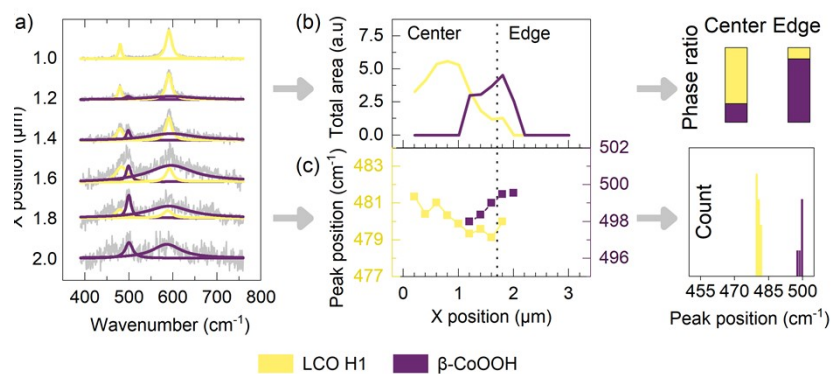**Fig. S10** Alternative model of Raman line scans sampling volume.

Fig. S11 The illustration of Raman line scans data processing for 1.8 V$_{RHE}$ 500 cycles sample.
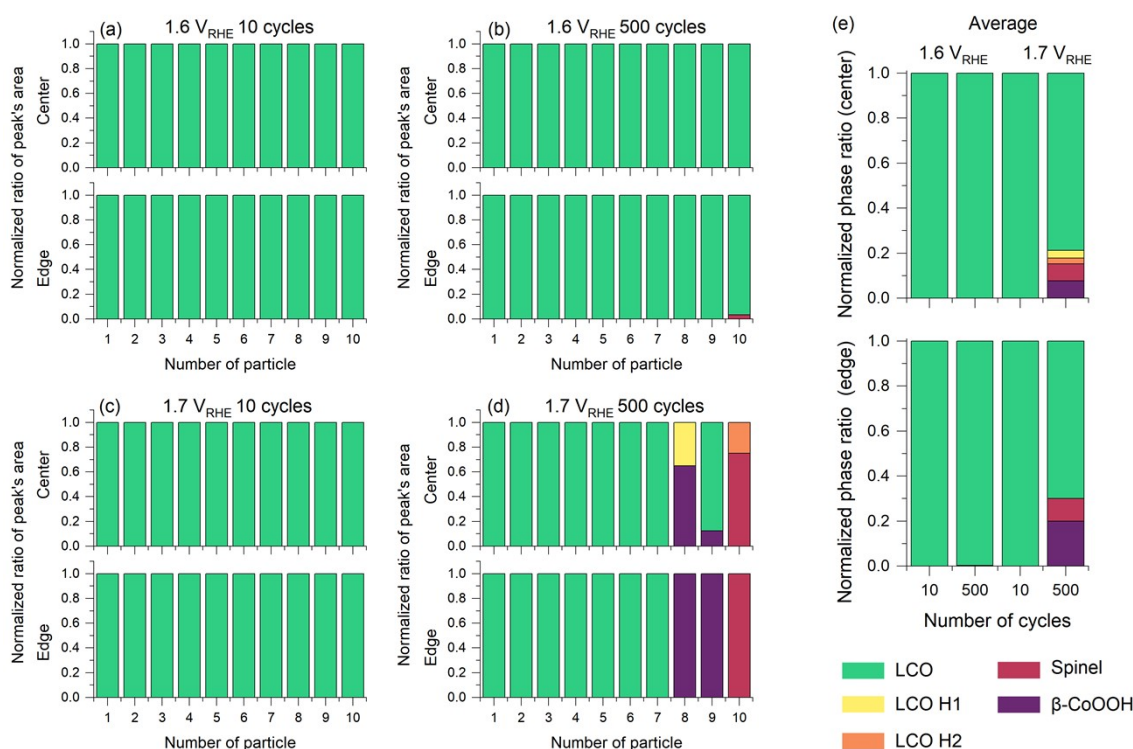
Fig. S12 Phase distribution from Raman line scans of LCO@1.6 after (a) 10 and (b) 500 cycles and LCO@1.7 after (a) 10 and (b) 500 cycles.
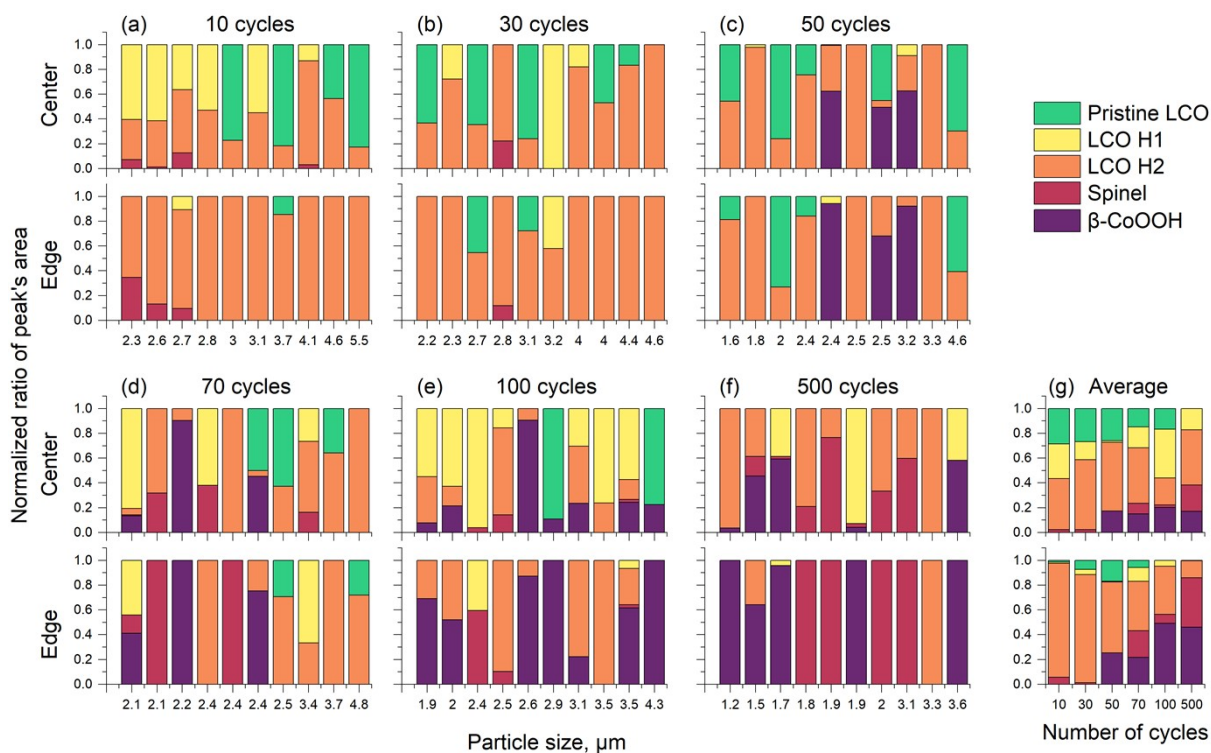

Fig. S13 Phase distribution from Raman line scans of LCO@1.8 V_{RHE} after different number of cycles.

To estimate the size of particles for the bar graph, we calculated their area in pixels using the standard Adobe Photoshop selection tool in optical images. We then converted the area from pixels to square nanometers and calculated the diameter using the formula for the area of a circle.
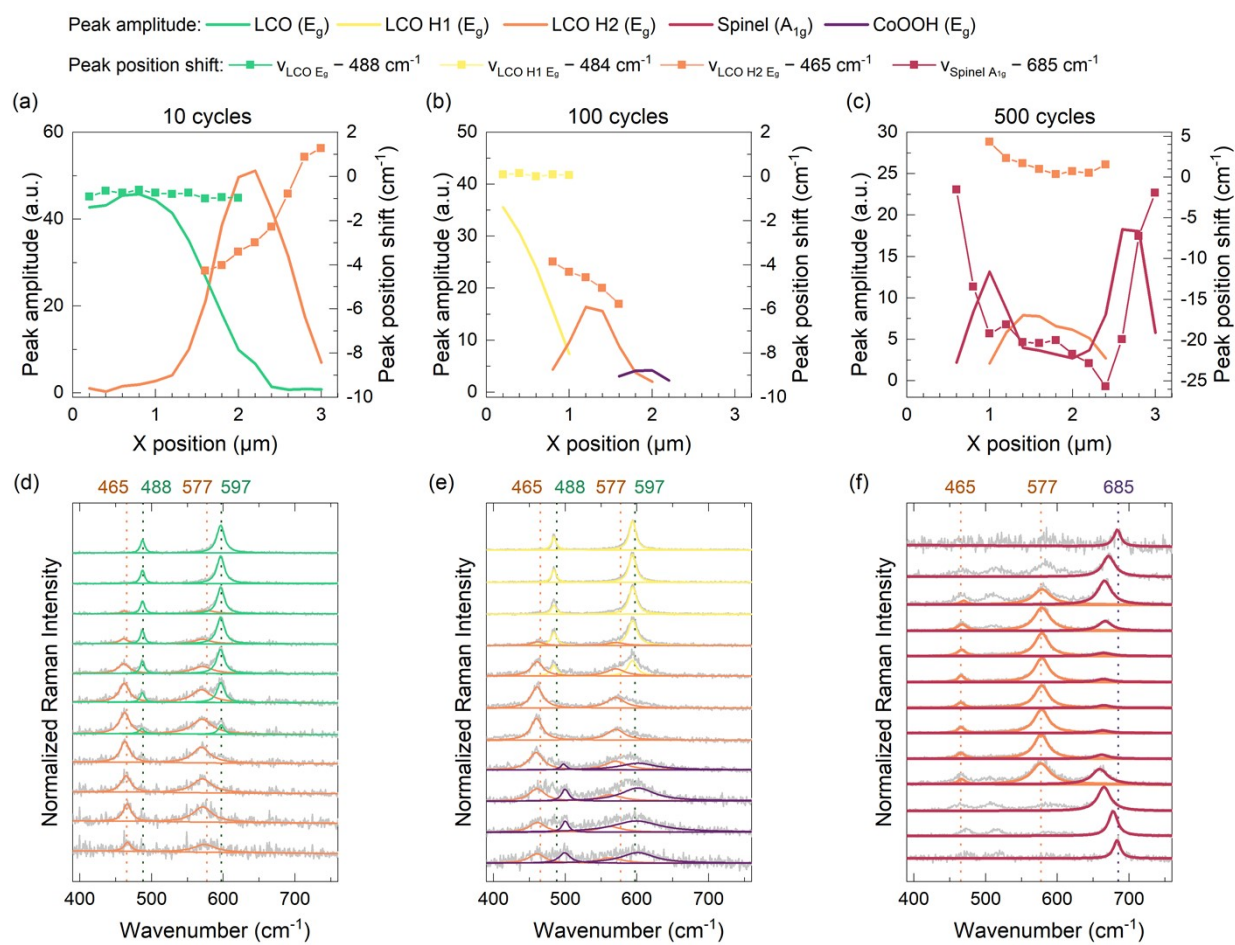
Fig. S14 (a)-(c) Peak parameters of corresponding (d)-(f) Raman line scan of LCO@1.8 particles.
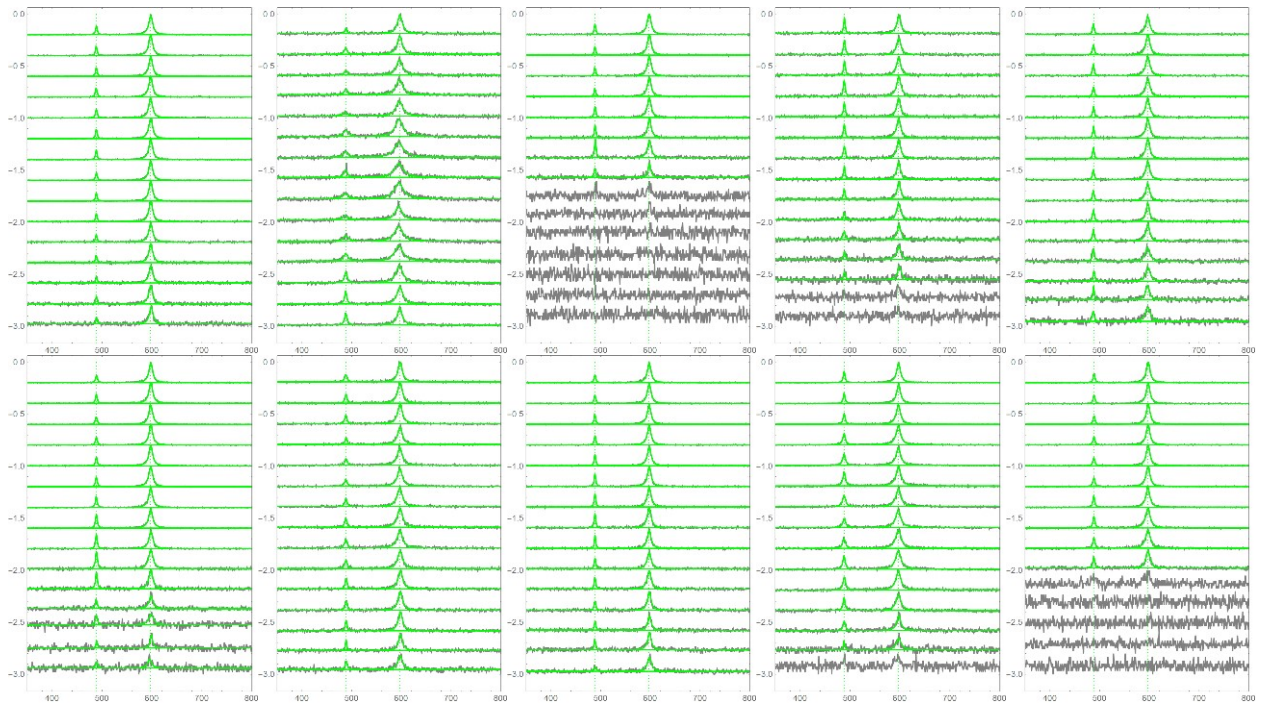
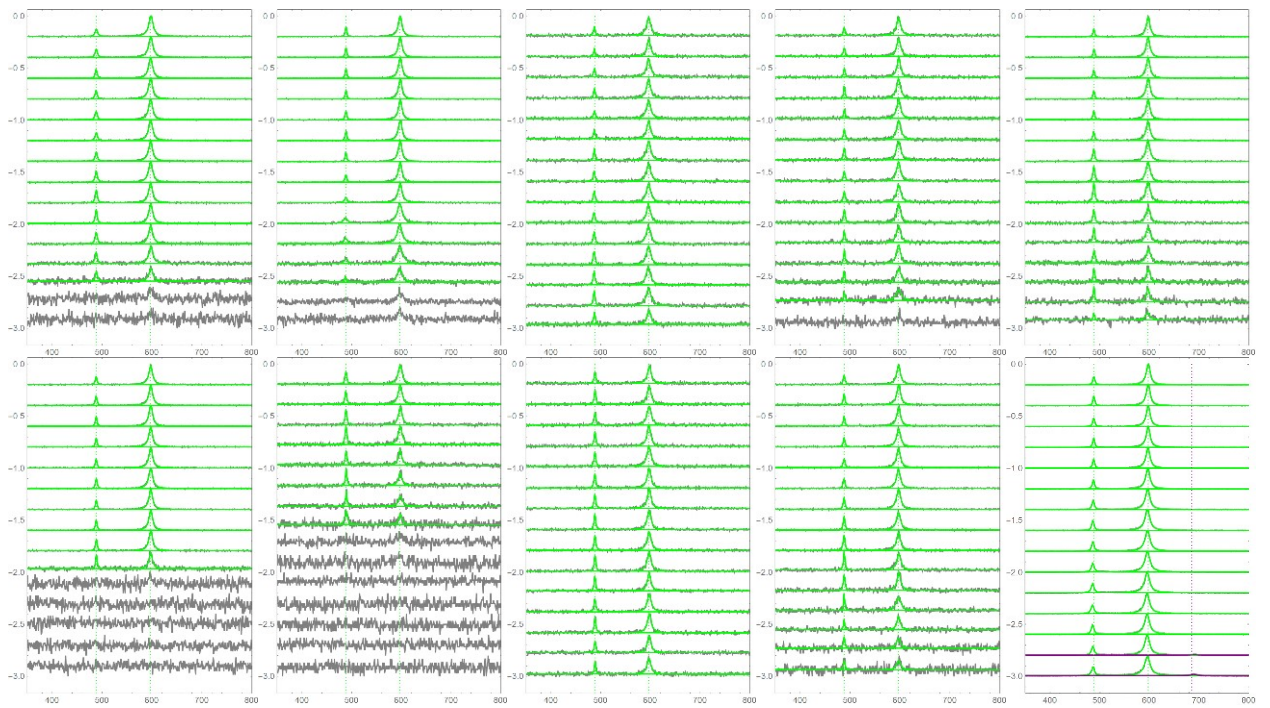**Fig. S15** Raman line scans of LCO@1.6 sample after 10 cycles.

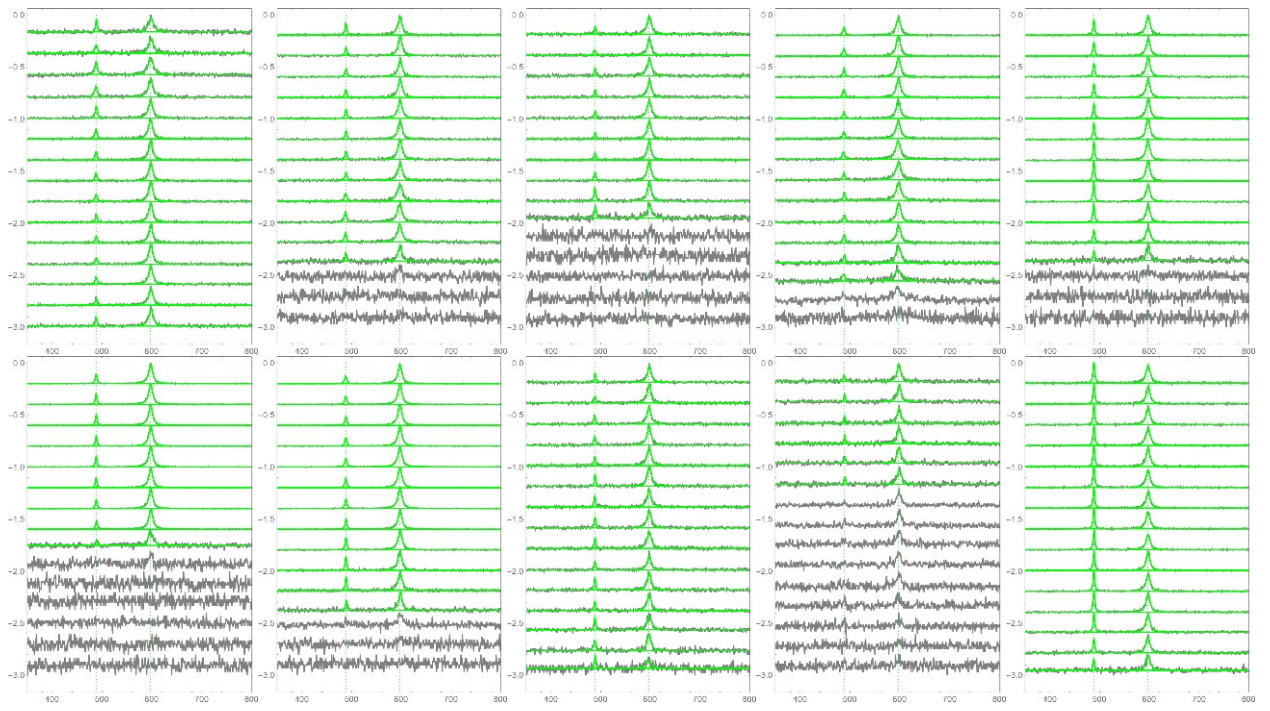**Fig. S16** Raman line scans of LCO@1.6 sample after 500 cycles.

Fig. S17 Raman line scans of LCO@1.7 sample after 10 cycles.
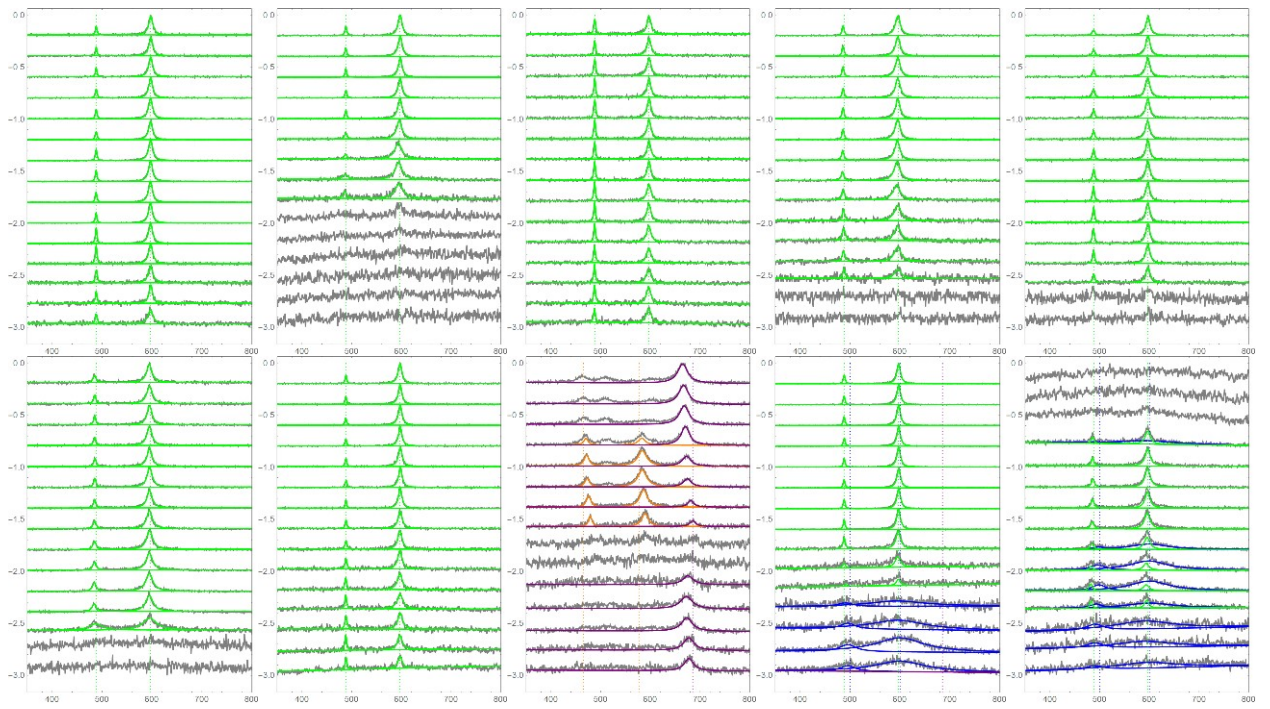

Fig. S18 Raman line scans of LCO@1.7 sample after 500 cycles.

Fig. S19 Raman line scans of LCO@1.8 sample after 10 cycles.

Fig. S20 Raman line scans of LCO@1.8 sample after 30 cycles.
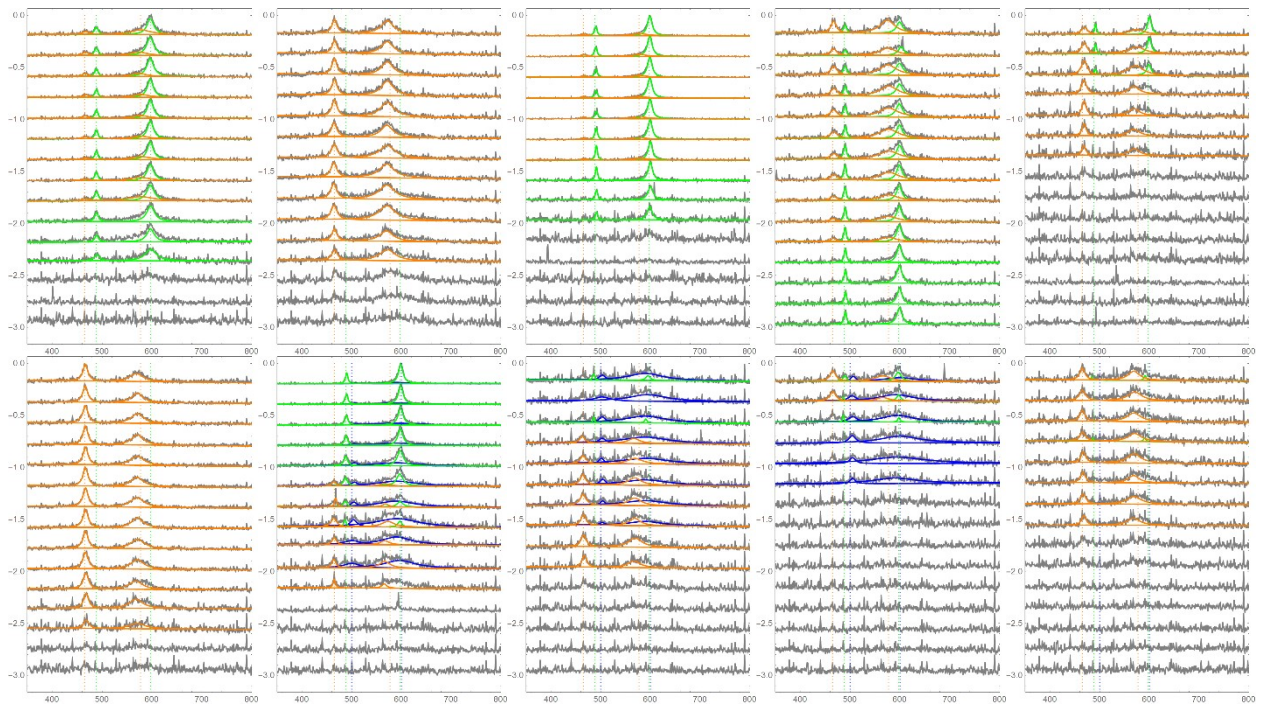
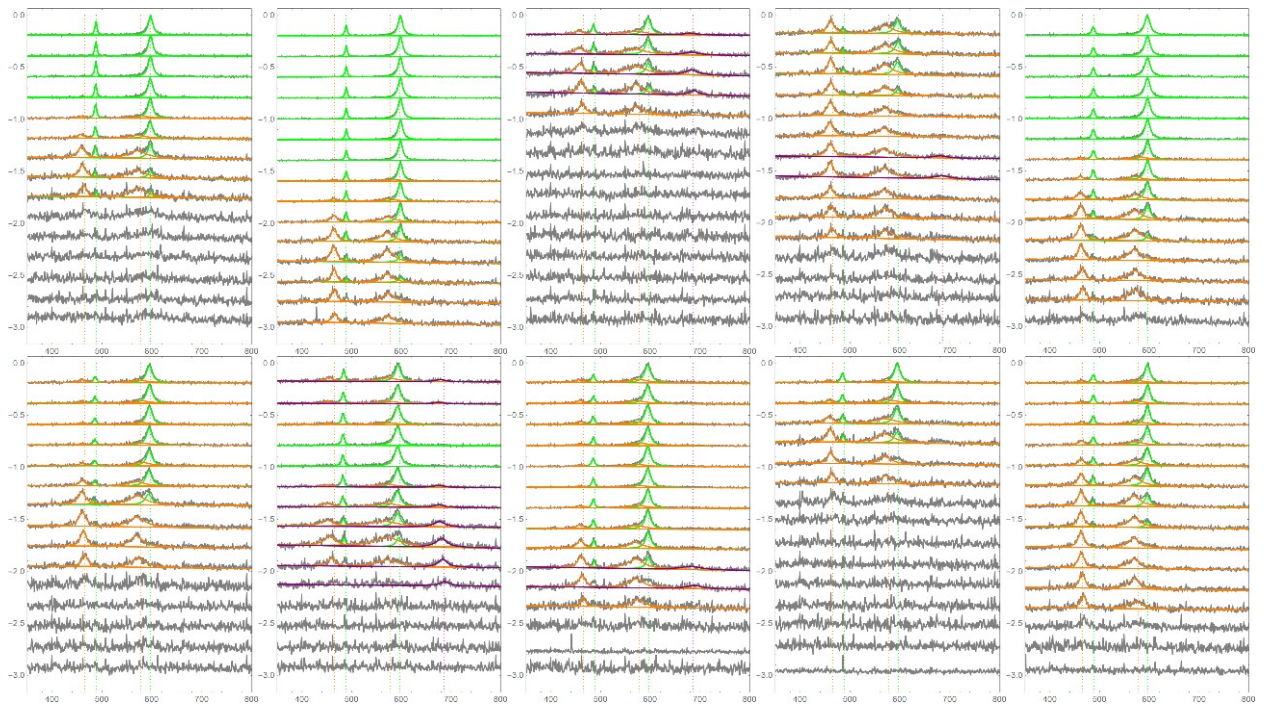**Fig. S21** Raman line scans of LCO@1.8 sample after 50 cycles.

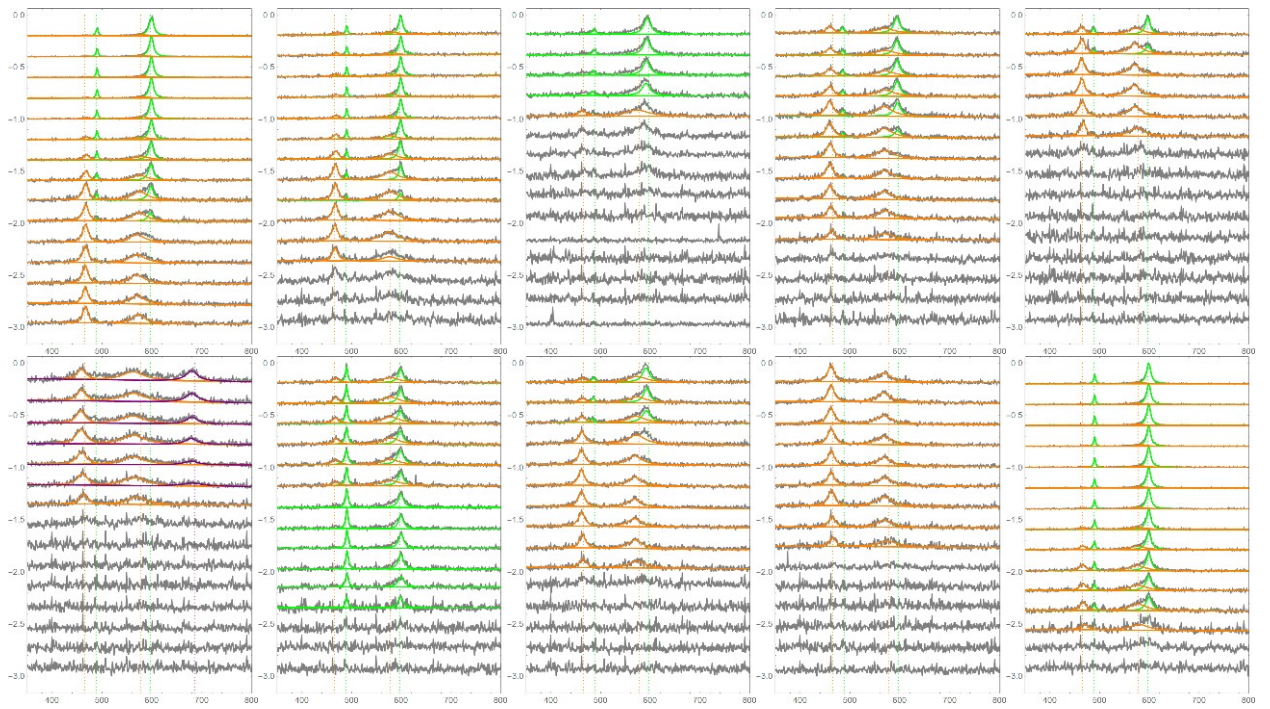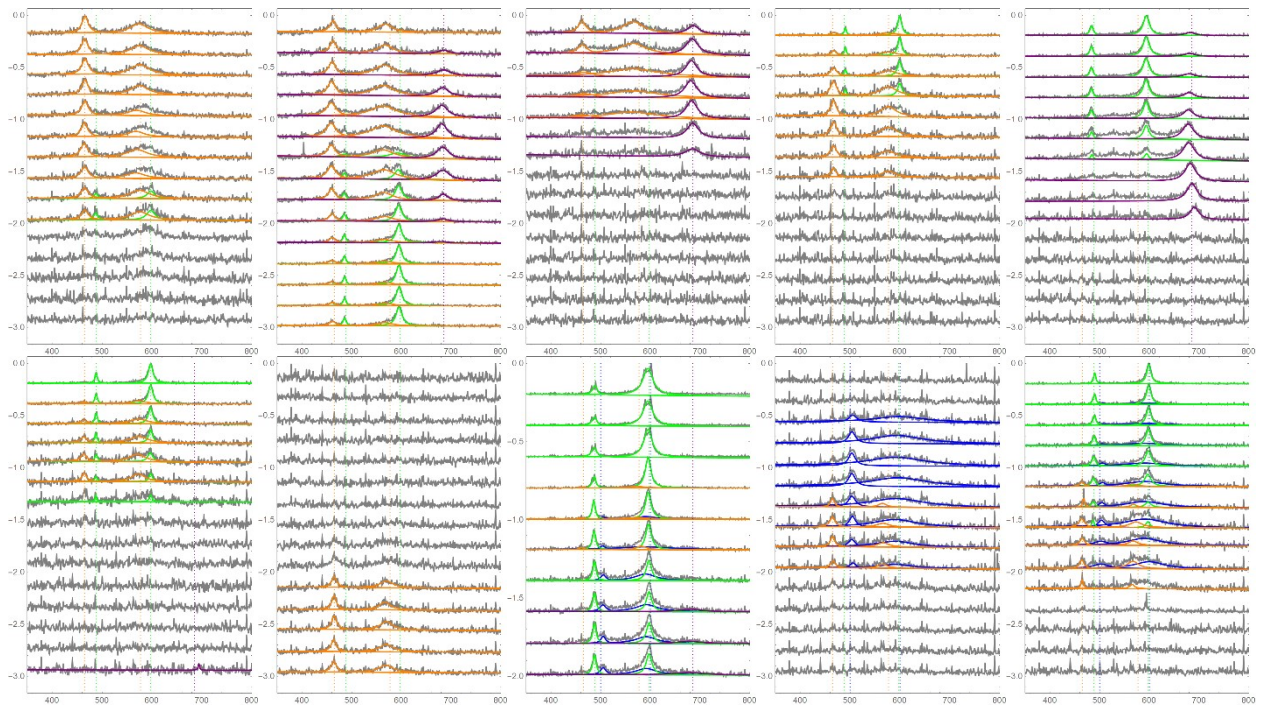**Fig. S22** Raman line scans of LCO@1.8 sample after 70 cycles.
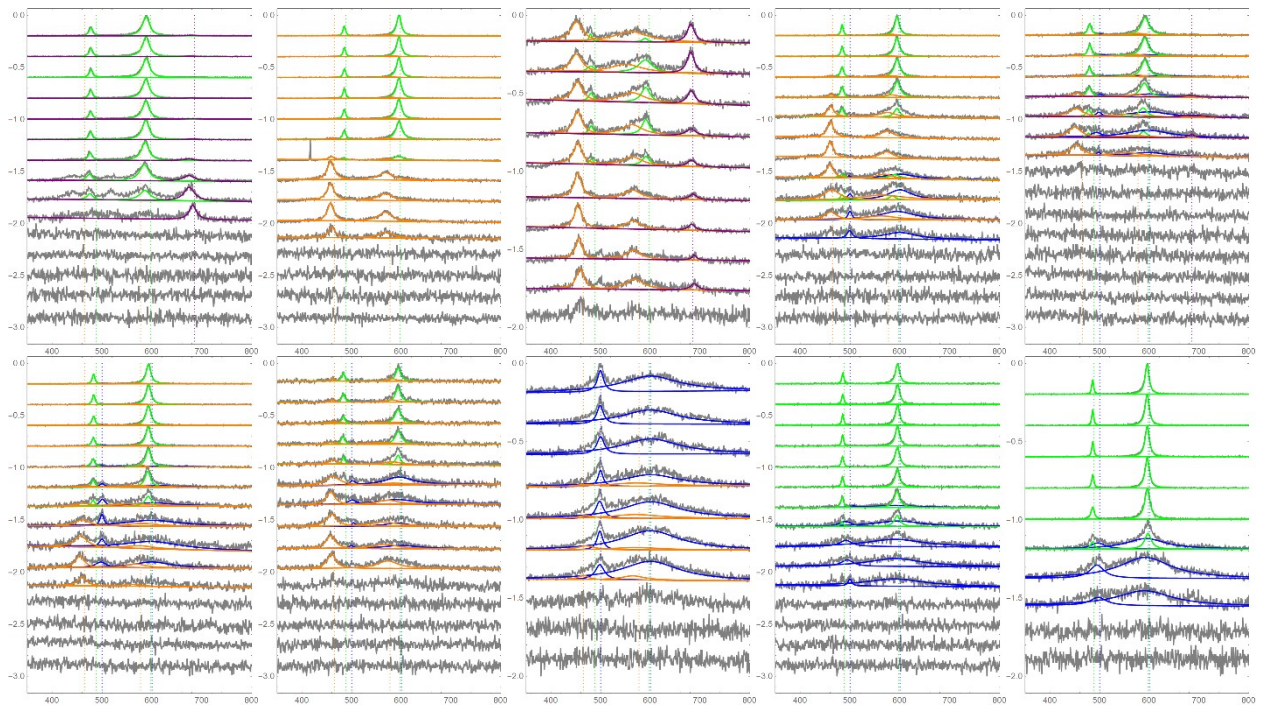
Fig. S23 Raman line scans of LCO@1.8 sample after 100 cycles.
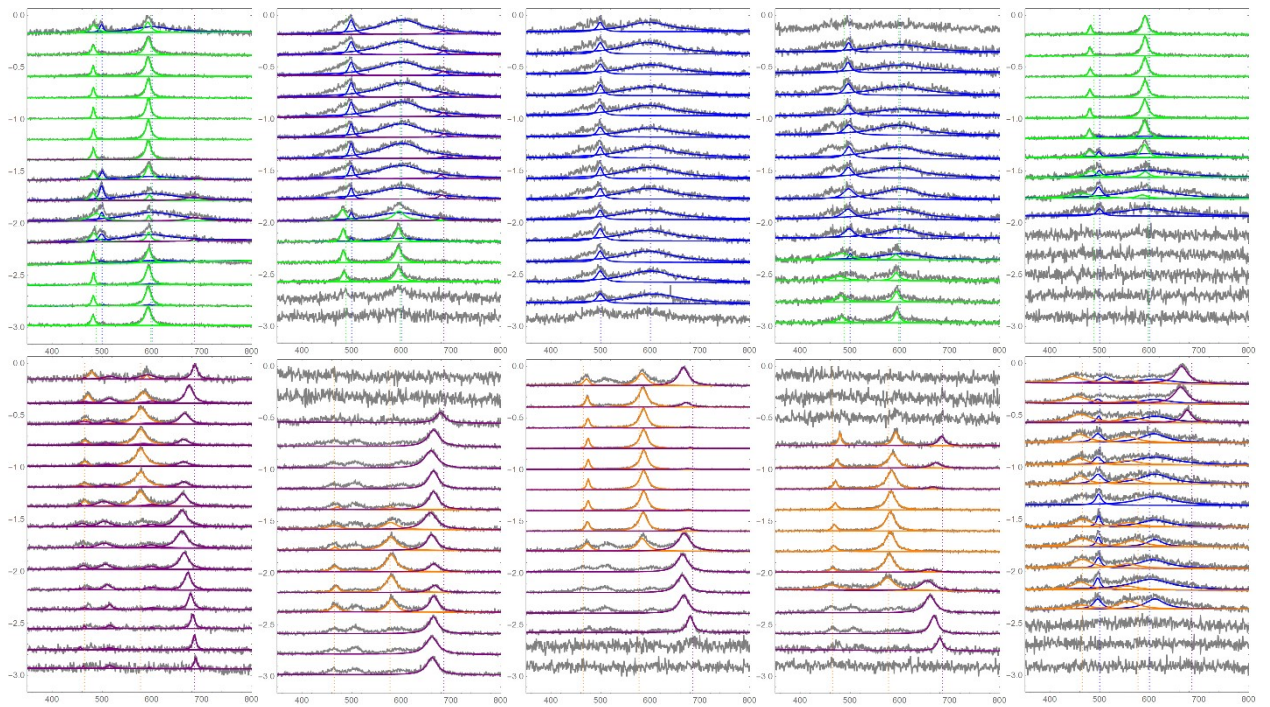
Fig. S24 Raman line scans of LCO@1.8 sample after 500 cycles.

The dashed lines for the presented scans have the following positions: LCO (green) - 488, 597 cm^{-1}; LCO H2 (orange) - 465, 577 cm^{-1}; Spinel (purple) - 685 cm^{-1}; CoOOH (blue) - 500, 600 cm^{-1}.

Fig. S25 Raman line scans of LCO@1.8 sample after 500 cycles and 24 hours of chronopotentiometry at 10 mA cm^{-2}.

Table S1 Inductively coupled plasma analysis results of LCO@1.8 after 500 cycles electrode and electrolytes.

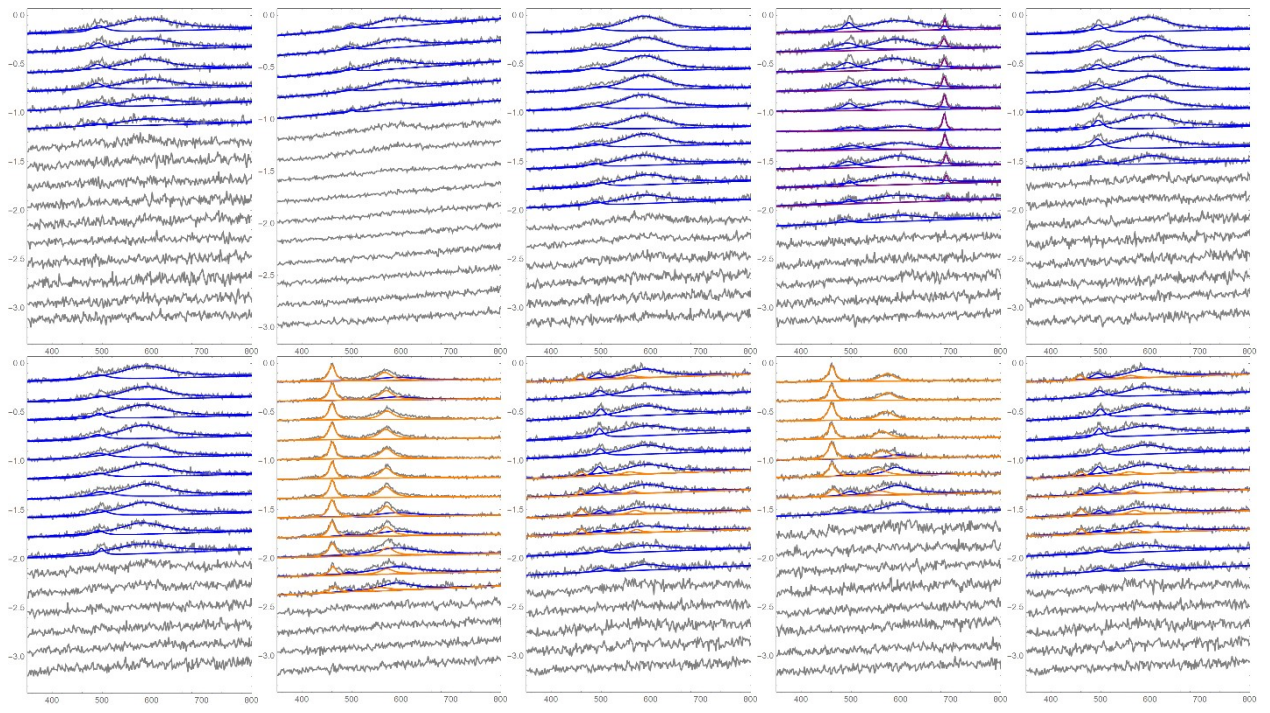| Sample		Li	Co
Pristine electrode*	Concentration (ppm)	0.87	7.90
	Molar ratio	0.94	1
LCO@1.8 500 cycles electrode*	Concentration (ppm)	0.32	5.50
	Molar ratio	0.49	1
Electrolyte before cycling**	Concentration (ppb)	1.6	Not detected
Electrolyte after cycling	Concentration (ppb)	1.8	Not detected

* measured by ICP-AES ** measured by ICP-MS

As suggested by the ICP-AES results, Li leaching from the LCO electrode cycled 500 times up to 1.8 V_{RHE} was confirmed. After cycling, the molar ratio of Li to Co in LCO reduced to 0.49:1, indicating a significant decrease in Li content compared to the pristine electrode. This demonstrates that the applied oxidation potential effectively caused Li leaching. Additionally, to detect the leached Li, the lithium concentration in the electrolyte before and after the protocol was confirmed via ICP-MS. The Co concentration in the electrolyte remained below the detection limit before and after the reaction, verifying no loss of Co through the cycling protocol. The concentration of Li increased by 2 ppb after the reaction, reflecting the Li leached from the LCO during the cycling protocol.

Table S2 Peak assignment for Co 2p XPS spectra.

Color of the peak in Fig. 3f-i	Green, eV	Yellow, eV	Purple, eV	Blue, eV	Pink, eV	Reference
Peak positions in our work	788.4-789.2	787.2	782.7-783	780.7-781	779.6-779.8	
Peak positions in the literature	789.1-790.7	786.3	782.4-783.8	781.2-781.7	779.6-780.7	
$LiCoO_2$	789.1	-	-	-	779.6	[2]
Delithiated $LiCoO_2$	789.6	-	-	781.5	779.8	[2]
CoOOH	790.3	-	782.4	781.3	780.3	[3]
CoOOH	789.9	-	783.8	781.7	780.4	[4]
Co_3O_4	789.8	785.5	782.5	781.2	779.9	[4]
$Co(OH)_2$	790.7	786.3	782.5	-	780.7	[4]

References

1   D. Uxa, E. Hüger, K. Meyer, L. Dörrer and H. Schmidt, *Chem. Mater.*, 2023, **35**, 3307–3315.

2   J. . Dupin, D. Gonbeau, H. Benqlilou-Moudden, P. Vinatier and A. Levasseur, *Thin Solid Films*, 2001, **384**, 23–32.

3   X. Cui, H. Zhao and Z. Li, *Anal. Bioanal. Chem.*, 2018, **410**, 7523–7535.

4   J. Yang, H. Liu, W. N. Martens and R. L. Frost, *J. Phys. Chem. C*, 2010, **114**, 111–119.